MODELING OF WIRE-ON-TUBE CONDENSERS FOR DOMESTIC REFRIGERATORS

Lima, R. S., rafaelsene@gmail.com
Seixlack, A. L., andre@dem.feis.unesp.br
Department of Mechanical Engineering - São Paulo State University - UNESP - CEP. 15385-000 - Ilha Solteira, SP – Brazil)

Abstract. *This work presents a numerical model to simulate the unsteady refrigerant fluid flow in wire-and-tube condensers, the kind widely used in vapor compression cycle based domestic refrigerator. The refrigerant fluid flow inside the condenser tube is complex and during the refrigeration system operation, long unsteady periods can occur as a consequence of, for example, starting or stopping the system, and variation of operating conditions of the system. During such periods, the flow regions can appear or disappear, making it difficult to model the flow. The present model considers the refrigerant flow inside the tubes divided in a superheated vapor flow, two-phase flow region and a subcooled liquid region. The refrigerant flow is considered as one-dimensional and the homogeneous flow model is employed for the two-phase flow region. The fundamental equations governing the flow through a wire-on-tube condenser are derived from the mass conservation, momentum and energy conservation laws. The energy conservation equation for the tube wall condenser is also solved to obtain the wall temperature distribution. The Finite Volume approach is used to discretize the governing partial differential equations and the resulting set of algebraic equations was solved by successive iterations. The model allows predictions of the steady and unsteady states refrigerant mass flow rate, pressure, quality, refrigerant and wall temperatures distributions along the tube as a function of the heat exchanger geometry and operating conditions. To validate the developed model, the results obtained were compared with results presented by other researcher available in literature.*

Keywords*: wire-on-tube condenser, transient flow, domestic refrigerator, heat exchanger, two-phase flow*

1. INTRODUCTION

The preoccupation with ecological issues is gaining attention nowadays, mainly in concern of atmospheric ozone layer, greenhouse effect, and requirement of new less pollutant sources of energy. In the field of refrigeration, such concerns have motivated several researches and big investment aiming at improving the thermodynamic efficiency and reducing manufacturing cost of the main refrigerator components such as evaporators, condensers, compressors and expansion devices. The fundamental subject of these researches is to analyze the behavior of devices when operating with refrigerant fluids which are less aggressive to the atmospheric ozone layer.

Several studies on condensers have been carried out with the aim of: (i) obtaining operating parameters of these kinds of heat exchangers, such as heat transfer coefficient, pressure drop along the flow and condenser capacity; (ii) developing new condensers well adapted to use alternative refrigerant fluids in place of CFCs and HCFCs; (iii) developing and characterizing the performance of new kinds and geometries of fins, and turbulence enhancers to intensify the heat transfer coefficient. A well-designed condenser will not only improve the energy efficiency, but will also reduce the space and material for a specific cooling capacity.

The condenser most widely applied in household refrigerators and freezers is the wire-and-tube condenser, known to be predominantly a natural convection heat exchanger. This condenser consists of a single steel tube that carries the refrigerant fluid and solid steel wires that serve as extended surface. The tube is wound into a single-passage serpentine shape and the wires are symmetrically spot welded to both sides in a direction perpendicular to the tubes, as illustrated in Fig. 1.

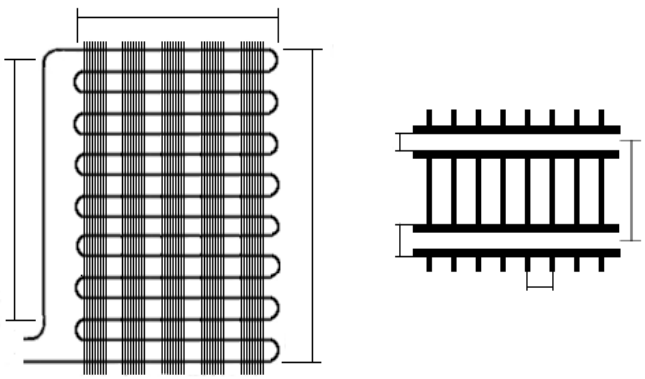

Figure 1 – Schematic and geometrical parameters of a wire-and-tube condenser.

On the left side of Fig. 1, L_e is the inlet region length (without wires), W_i and W_e are respectively the width and height of the condenser. On the right side of the figure, d_i and d_e represents the inner and outer tube diameters, respectively. The wire and tube pitches are represented by p_{wi} and $p_{t,}$ respectively.

The refrigerant fluid flow inside the condenser tube is complex and generally, due to phase change, it is possible to find three regions: a superheated vapor flow, a two-phase flow (liquid-vapor) and a subcooled liquid flow region. Furthermore, during the refrigeration system operation, long unsteady periods occur as a consequence of, for example, starting or stopping the system, starting or stopping the compressor, and variation of system operating conditions. During such periods, one of those flow regions may appear or disappear, making it more difficult to model the flow.

The refrigerant flows along L_e as superheated vapor and in certain condenser tube lengths, convective condensing starts until the refrigerant leaves the condenser as subcooled liquid or as a saturated two-phase mixture. The heat is transferred from the tube wall to the external environment by radiation and natural convection.

Theoretical and experimental studies dealing with different aspects of the performance of wire-and-tube condensers have been the subject of several research works, such as reported by: Tagliafico and Tanda (1997), Hermes and Melo (2008), Quadir *et al*. (2002), Bansal and Chin (2003), Melo *et al.* (2004) and Ameen *et al.* (2005).

Tagliafico and Tanda (1997) developed a theoretical-experimental study to analyze the radiation and natural convection heat transfer characteristics of the wire-and-tube condenser. These researchers proposed a semi-empirical correlation for the natural convection contribution. The radiation component was calculated theoretically and subtracted from the total heat transfer rate. It was reported that the proposed correlation was predicted with a 6% standard deviation.

Melo *et al*. (2004) carried out an experimental study on of the performance of the wire-and-tube condenser under various operating conditions to investigate the role played by the confining walls on the heat transfer from this unit. The experiments were carried out using a specially developed testing apparatus comprising a test section to vary the heat exchanger position in relation to the adjacent surfaces. The results showed that the condenser performance is strongly affected by the gap between the refrigerator and the rear wall.

Quadir *et al*. (2002), on the other hand, developed a model using the finite element method to analyze the performance of a wire-and-tube condenser under natural cooling condition. It was reported that the model was validated successfully against the available results where latent heat transfer or sensible heat transfer takes place.

A numerical model for simulating the dynamic behavior of household refrigerators was developed by Hermes and Melo (2008). Each of the refrigerator components: compressor, evaporator, wire-and-tube condenser, cabinet and capillary tube-suction line heat exchanger was modeled. The condenser model was based on the mass conservation, momentum and energy laws written in the differential form. The author reported that the model was in close agreement with results obtained by Klein (1998) for the steady state. For the transient model, the simulation was performed with imposed boundary conditions based on experimental results of pull-down tests, which allowed a qualitative analysis of the model and of the viability of its numerical solution.

Bansal and Chin (2003) presented the modeling and experimental results of wire-and-tube condensers. A condenser was experimentally tested in a real refrigerator under some operating conditions. The computer model was developed using the finite element method and variable conductance approach along with a combination of thermodynamic correlations. The model was validated by experimental results obtained by the same authors. The condenser capacity per unit weight was optimized using a variety of wire and tube pitches and diameters. The results showed that the condenser design with the optimum capacity/weight ratio gains 3% in capacity and 6% in weight reduction.

A numerical analysis and experimental investigation into the performance of a wire-and-tube condenser of a retrofitted refrigerator was developed by Ameen *et al.* (2005). The numerical model considered a condenser under various operating conditions of natural convection using the finite element method. In terms of initial and final phase change point locations, the predicted and experimental results were found to agree within ±10%.

The present paper aims at presenting a model to simulate the unsteady behavior of a household refrigerator wire-and-tube condenser considering the refrigerant flow along the tube. The model also considers that the heat transfer from the outer surfaces of the wires and tubes to the surrounding air takes place by natural convection and radiation. The refrigerant flow is considered to be one-dimensional and the homogeneous flow model is employed for the two-phase flow region, i.e., the hydrodynamic and thermal equilibrium between the phases are considered.

The mass conservation, momentum and energy conservation equations for the refrigerant flow were solved to evaluate the distributions of mass flux, pressure and temperature of the refrigerant, respectively. The energy conservation equation for the tube wall was also solved to determine the wall temperature distribution.

The governing differential equations were discretized using the Finite Volume approach and the resulting set of algebraic equations was solved by successive iterations. The model allows for the prediction, in steady and unsteady states, of the refrigerant mass flow rate, pressure, quality, refrigerant and wall temperatures distributions along the tube, as a function of the heat exchanger geometry and operating conditions. Besides, the model can be used for designing and predicting the performance of a wire-and-tube condenser. The model was later analyzed and the results obtained were compared with those available in the literature.

2. MATHEMATICAL MODEL

In the present model, the flow along the wire-and-tube condenser is divided in three distinct regions: a superheated vapor flow, two-phase flow and a subcooled liquid flow region. The condenser is divided in two sections: the inlet section, L_e, without wires, and the wired section, which constitutes the largest part of heat exchanger with width W_i and height is W_e (see Fig. 1). The flow pressure drop inside the tube is considered since it can represent significant portion in the initial stages after the compressor start-up (Hermes and Melo, 2008).

The assumptions made in the present model are: (a) the condenser is a straight and horizontal tube with constant diameter, i.e., the effects of coil curvature are neglected; (b) the wires are uniformly spaced; (c) the flow and heat transfer are one-dimensional; (d) the refrigerant is an oil free Newtonian fluid ; (e) mechanical equilibrium is valid, i.e., the pressure is uniform in any cross-section of the tube and the effects of surface tension are neglected; (f) there is no axial heat conduction, viscous dissipation of energy, nor variation of potential energy in the flow along the condenser and the flow pulsation; (g) heat conduction in the tube wall is axially distributed and radially lumped; (h) the surrounding temperature is constant; (i) the radiation heat transfer equation between the pipe wall and the surrounding is linear, (j) the thermophysical properties of the tube wall are constant; (k) the two-phase flow along the condenser tube is homogeneous, i.e., the flow is mathematically treated as a pseudo single-phase flow whose properties are determined by the quality of liquid-vapor mixture and by the properties of each phase. Therefore, both phases have the same velocities, pressures and temperatures in any tube transverse section.

Based on the above assumptions, the governing equations for the in tube refrigerant fluid are given by:

(i) Mass conservation:

$$\frac{\partial \rho}{\partial t} + \frac{\partial G}{\partial z} = 0 \tag{1}$$

where $G = \rho u$ is the refrigerant mass flux [kg/m^{2}s]. In the two-phase flow, $\rho = \rho_l + \alpha(\rho_v - \rho_l)$ where α is the void fraction (ratio of the portion of the cross-sectional area occupied by the vapor to the total cross-sectional area).

(ii) Momentum equation:

$$\frac{\partial G}{\partial t} + \frac{\partial\ Gu}{\partial z} = -\frac{\partial p}{\partial z} - F_z \tag{2}$$

where $F_z = (fG^2 / 2\rho d_i)$ is the force per unit volume due to the friction between the refrigerant and the tube wall.

(iii) Energy conservation for the refrigerant flow:

An energy balance in the refrigerant flow results in,

$$\frac{\partial\ \rho h_o}{\partial t} + \frac{\partial\ Gh_o}{\partial z} = \frac{\partial p}{\partial t} - \frac{H_i\ \ T_r - T_{wc}\ \ P_i}{A_i} \tag{3}$$

where $h_o=(h+u^2/2)$ is the specific stagnation enthalpy, [J/kg], $P_i = (\pi d_i)$ is the inner tube perimeter and $A_i = (\pi d_i^2 / 4)$ is the cross-sectional area of the tube [m^2]. In the two-phase flow region: $h = [h_l + x(h_v - h_l)]$.

The energy conservation for the tube wall is given by:

$$(\rho c)_{wc} \frac{\partial T_{wc}}{\partial t} = k_{wc} \frac{\partial^2 T_{wc}}{\partial z^2} + \frac{P_i}{A_{cs}} H_i\ \ T_r - T_{wc}\ \ - \frac{P_e}{A_{cs}}\ \ T_{wc} - T_a\ \ (H_{rad} + H_e) \tag{4}$$

where $A_{cs} = [\pi(d_e^2 - d_i^2)/4]$ is the cross-sectional area of the tube wall [m^2], $H_{rad} = \sigma\varepsilon(T_{wc} + T_a)(T_{wc}^2 + T_a^2)$ is the radiation heat transfer coefficient [W/m^{2}K], σ = 5,67x10^{-8} [W/m^2 K^4] is the Steffan-Boltzman constant and $P_e = (\pi d_e)$ is the outer perimeter of the tube [m]. The tube wall material is steel (ρ_{wc}=7850 kg/m^3; c_{wc}=477 J/kgK; k_{wc}=50 W/mK; ε=0.92)

Therefore, the proposed model consists of Eqs. (1) to (4) which should be solved to give the distributions of G, p, h_0 and T_{wc}, respectively. In addition the model uses the following closure relationships: (i) for the friction factor, the Churchill (1977) correlation is used in all flow regions. The Reynolds number is evaluated using the mean two-phase viscosity equal to the liquid-phase viscosity in two-phase flow; (ii) for the H_i in subcooled and superheated regions, the Gnielinski (1976) correlation is applied; (iv) for the H_i in two-phase flow, the Shao and Granryd (1995) correlation is

used; (v) for the H_e in the inlet region, the LeFevre and Ede (1956) correlation is employed; and (vi) for the H_e in wired region, Tagliafico and Tanda (1997) correlation is used. Lastly, the refrigerant thermo-physical properties were determined using the software REFPROP 6.01 (McLinden *et al.*, 1998).

2.1. Initial and Boundary Conditions

In Figure 2, the line between the points 1 to 4 is a schematic representation of a common situation of the flow along a wire-and-tube condenser. The regions located between points 1-2, 2-3 and 3-4 correspond to the superheated flow, two-phase flow and subcooled flow regions respectively. The governing equation, Eqs. (1) to (3), are first order partial differential equations and, therefore, require one initial and one boundary condition to be solved while the governing Eq. (4) is a second order partial differential equation and therefore requires one initial and two boundary conditions to be solved.

In the superheated vapor and subcooled liquid regions, the temperature and density are determined as functions of the pressure, $T_r = T_r(p,h)$ and the enthalpy, $\rho = \rho(p,h)$. The solution algorithm for the governing equations was written in language C. Since the computational program, REFPROP 6.01 is written in language FORTRAN, an application was elaborated in language C++ to associate the C and FORTRAN languages. All results obtained in the present work were plotted using the graphics tool *Pylab*, a software program used in creating two-dimensional graphic draw ups for the computational language Python.

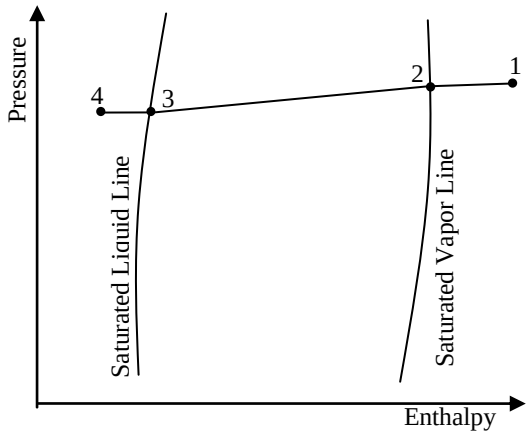

Figure 2 – Schematic pressure-enthalpy diagram representing the thermodynamic states of the refrigerant fluid along the wire-and-tube condenser.

At the condenser inlet, *z=0* (state 1 in Fig. 2), the boundary conditions are: the refrigerant mass flux (G_1) and the thermodynamic state of the refrigerant (p_1,T_1). All thermodynamics properties at that point are h determined from the known temperature and pressure at state 1. The wall temperature of the condenser at the inlet is considered equal to $T_{r,1}$ and a null wall temperature gradient is adopted at the condenser outlet. Thus, the boundary conditions at the inlet of the condenser are given by,

$$z = z_1 = 0 \quad \begin{cases} G = G_1 \qquad p = p_1 \qquad T_r = T_{wc} = T_1 \\ \\ \rho = \rho\ (p_1, T_1) \qquad\qquad h = h\ (p_1, T_1) \end{cases} \tag{5}$$

The two-phase flow region inlet, state 2 in Fig. 2, is characterized by comparing the refrigerant pressure calculated and the saturation pressure relative to refrigerant temperature, $p_{sat}(T_r)$, obtained using REFPROP 6.01. The two-phase region outlet is assumed for the refrigerant quality, that is, the position along the tube where x = 0 and the thermodynamic properties are those of the saturated liquid state at the inlet of the subcooled liquid region.

The transient behavior of the condenser is analyzed according to Hermes and Melo (2008) by imposing time dependent boundary conditions, generated from the steady state results performed by Klein (1998), and the experimental results of pull down testes performed by Hermes and Melo (2008). Such tests consist of monitoring the evolution of the transient pressure, temperature and power consumed by the refrigeration system from the start-up to the steady–state. According to Hermes and Melo (2008), in general, the boundary conditions imposed to simulate the start-

up can be represented as: $\beta = \beta_\infty + \beta_o - \beta_\infty \; e^{-t/a}$, where β is generic dependent variable, β_o is the initial value of the variable calculated according to the pressure equalization system and the ambient temperature, β_∞ is the value of β under steady–state conditions and *a* is a time constant. Notice that the function given by β is increasing for $\beta_o < \beta_\infty$ and decreasing for $\beta_o > \beta_\infty$, with an asymptotic behavior with respect to β.

3. SOLUTION METHODOLOGY

The numerical solution of the refrigerant flow governing equations, Eqs. (1)-(3), was carried out by using the Finite Volume method and the resulting set of algebraic equations was solved using a one-way march procedure by successive iterations. The domain was divided in *m* control volumes with the discretization nodes located at the inlet and outlet section of these volumes (see Fig. 3). This numerical procedure is similar in many aspects to that presented by Escanes *et al.* (1995) and the equation used in this work to generate the computational grid is the same presented by Escanes *et al.* (1995). In almost all cases analyzed, the mesh used for the steady state solution was composed of 300 volumes and of 200 volumes for transient solution.

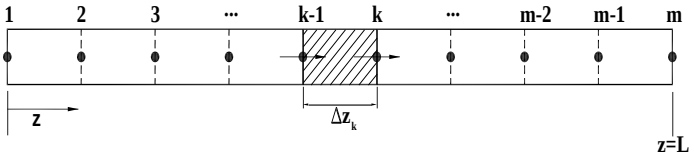

Figure 3 – Control volumes along the discretized one-dimensional domain.

The governing equations were integrated over time and space along each control volumes of length, Δz. A first order completely implicit scheme was employed to integrate the transient terms in order to avoid negative coefficients and to ensure numerical stability of the solution procedure independent of the time step employed. A first order approximation was also employed for the integration of the source terms over the control volume. Accordingly, the integration procedure is approximated by,

$$\bar{\beta} = \frac{1}{\Delta z} \int_{z_{k-1}}^{z_k} \beta dz \cong \beta_k \tag{6}$$

where β represents a generic dependent variable per unit of mass or a generic source term of some of the governing equations.

Thus the transient terms are discretized using the approximation: $\partial\beta / \partial t = [(\beta - \beta^o)] / \Delta t$, where Δt is the time interval [s]. The superscript ^{o} denotes the previous time step value of the variable β while the subscript *k* represents the node located at the outlet section of the control volume (see Fig. 3).

Following above described approach after discretization, Eqs. (1)-(3) take, respectively, the forms,

$$G_k = G_{k-1} - \left(\rho_k - \rho_k^o \right) \frac{\Delta z}{\Delta t} \tag{7}$$

$$p_k = p_{k-1} - G_k u_k + G_{k-1} u_{k-1} - (F_z)_k \Delta z_k - \frac{(G_k - G_k^o)}{\Delta t} \tag{8}$$

and

$$h_{o,k} = \frac{(Gh_o)_{k-1} - q''_{i,k} \frac{P_i}{A_i} \Delta z_k + \left[(p_k - p_k^o) + (\rho h_o)_k^o \right] \frac{\Delta z_k}{\Delta t}}{\rho_k \frac{\Delta z_k}{\Delta t} + G_k} \tag{9}$$

where $q''_i = H_i (T_r - T_{wc})$.

The heat conduction equation for the tube wall, Eq. (4), was also solved using the Finite Volume method. Thus, the Eq. (4) w integrated over time and space along each control volume of length Δz of the tube wall and the derivatives on the face of the control volume were evaluate using the central difference scheme. After discretization, Eq. (4) assumed the form,

$$T_{wc,k} = \frac{\dfrac{T_{wc,k+1}}{\Delta z_{k+1}} + \dfrac{T_{wc,k-1}}{\Delta z_{k-1}} + \dfrac{T^{o}_{wc,k}\Delta z_k}{\alpha_{wc,k}\Delta t} + b_k}{a_k} \tag{10}$$

where $\alpha_{wc} = (k/\rho c)_{wc}$ is the thermal diffusivity of the wall condenser,

$$a_k = \frac{2}{\Delta z_k} + \frac{\Delta z_k}{\alpha_{wc,k}\Delta t} + \frac{P_i H_{i,k}\Delta z_k}{k_{wc}A_{cs}} + \frac{P_e}{k_{wc}A_{cs}}\left(H_{rad} + H_e \right|_k \Delta z_k \tag{11}$$

and,

$$b_k = \left[\frac{P_i}{k_{wc}A_{cs}} H_{i,k}T_{r,k} + \frac{P_e}{k_{wc}A_{cs}} T_a \left(H_{rad} + H_e \right|_k \right] \Delta z_k \tag{12}$$

Given the geometry and operating conditions, the proposed model can be used to calculate the transient distribution of mass flux, pressure, stagnation enthalpy and the temperature of the wall condenser. The computation procedure is iterative because the equations depend on the mass flow rate. Hence, at each time step, by assuming a value for p at the condenser inlet and the other known operating conditions, the discretized equations were solved by successive substitution along the condenser. The dependent variables G, p, h_o e T_{wc} were then calculated for each discrete nodal point in the computational grid until the relative error between two consecutive iterations were less than 10^{-6} throughout the domain.

After solving the governing equations for the value of p assumed, the calculated refrigerant mass flux at condenser outlet, G_o, was then compared with its value at the condenser output set as boundary condition, G_o^*. The pressure was then adjusted iteratively, using the secant method until $\left|G_o - G_o^*\right| < 10^{-4}$.

4. STEADY STATE RESULTS

The steady state model presented was validated using the experimental results available in the open literature. The lack of some information on the condenser geometry and also on the operation conditions in most of the available works reduces the number of works that can be used for the validation of theoretical models.

First, the computational code was tested for the steady state condition using three particular cases with the same operating conditions considered by Hermes and Melo (2008) shown in Tab. 1. The solution procedure for these cases has already been presented in the previous item using a time increment of 10^4 s.

Table 1 – Operating conditions for the steady state analysis Hermes and Melo (2008).

Operating conditions	Case 1	Case 2	Case 3
Ambient temperature [°C]	32	43	54
Mass flux [kg/m^{2}s]	46.3	56.4	70.1
Inlet pressure [kPa]	1180	1553	2005
Inlet temperature [K]	74.9	89.7	102.6

The geometrical parameters of the condenser analyzed, according to Fig. 1, were: L_e = 1.5 m; W_e = 84 cm; W_i = 47 cm; d_i = 3.34 mm; d_e = 4.76 mm; p_{wi} = 4.52 mm; p_t = 56 mm. The remaining geometric parameters, not shown in Fig. 1, were: wired tube length = 7.5 m; number of coil passes = 15; number of wires = 104; wire diameter = 1.5 mm; wire length = 85.5 mm. The thermophysical properties of tube wall were: ρ_c = 7850 kg/m³; c_{wc}: 477 J/kgK; k_{wc} = 50W/mK; ε = 0.92.

Table 2 shows a comparison between the results obtained by the present model for a computational mesh of 300 volumes, and the results obtained by Hermes and Melo (2008). As can be perceived from the Table, the results obtained are in very close agreement with those of Hermes and Melo (2008).
From the results, it is easy to observe that the relative differences between the proposed model condenser capacity and that given by Hermes and Melo (2008) are within 1.0 and 3.5% range while for the refrigerant temperature in the condenser outlet, this difference is within 0.2 and 2.1% range. For case 1, the present model results in a subcooling in the condenser outlet of ΔT_{sub} = 3.7 ° C while for the Hermes and Melo (2008) model subcooling in the condenser outlet occurs at ΔT_{sub} = 3.3 ° C. For cases 2 and 3 the relative difference between the outlet qualities based on the present model and Hermes and Melo (2008) model are respectively 24.2% and 14.4%. For case 2, notice a difference of 24.2% between the outlet qualities, probably due to the small order of magnitude of both absolute values.

Table 2 – Comparisons between this model and that proposed by Hermes and Melo (2008).

Parameter	Result	Case1	Case 2	Case 3
Condenser capacity [W]	Present model	78.2	87.8	101.7
	Hermes and Melo[2]	79.0	88.8	98.3
	AD*	-0.8	-1.0	3.4
	RD (%)**	-1.0	-1.1	3.5
Outlet temperature [ºC]	Present model	41.7	56.5	67.4
	Hermes and Melo[2]	42.6	56.6	67.6
	AD*	-0.9	-0.1	-0.2
	RD (%)**	-2.1	-0.2	-0.3
Outlet quality (%)	Present model	ΔT_{sub}=3.7 ºC	2.5	13.5
	Hermes and Melo[2]	ΔT_{sub}=3.3ºC	3.3	11.8
	AD*	ΔT_{sub}=0.4ºC	-0.8	1.7
	RD (%)**	-	-24.2	14.4

* Absolute Difference; ** Relative Difference.

The term F_z present in the momentum equation, Eq (2) deserves attention since it can cause a pressure drop of approximately 200 kPa (0.2 bar) in the initial instants after the compressor start-up (14). However, in steady state, Klein (1998) obtained values of pressure drop much lower, around 2 kPa (0.02 bar), since the refrigerant mass flow rate is lower.

The Churchill (1977) correlation was used to evaluate the friction factor, f in the single phase regions. Four procedures were analyzed in the two-phase region: (a) assuming the mean two-phase viscosity is equal to the liquid viscosity ($\bar{\mu} = \mu_l$) to evaluate f; (b) using the McAdams *et al.* (1942) correlation for the mean two-phase viscosity $\bar{\mu}$ to evaluate f; (c) using the Lockhart-Martinelli (1949) correlation to calculate the two-phase frictional multipliers ϕ_l^2 and ϕ_v^2 ; and (d) using the Grönnerud correlation, *apud* Ould Didi *et al.* (2002) to calculate the two-phase frictional multiplier ϕ_l^2 . The refrigerant pressure and temperature distributions calculated using the correlations analyzed, for Case 2 of Tab. 1, against the normalized distance along the condenser, z / L (ratio of the position along the condenser to total condenser length) are shown in Figs. 4 and 5 respectively. Notice that in the superheated vapor region, $(z/L) \leq 0.25$ (Figs. 4 and 5), there is only one curve for pressure and temperature distributions each. This is because the friction factor in that region was evaluated using only the Churchill (1977) correlation.

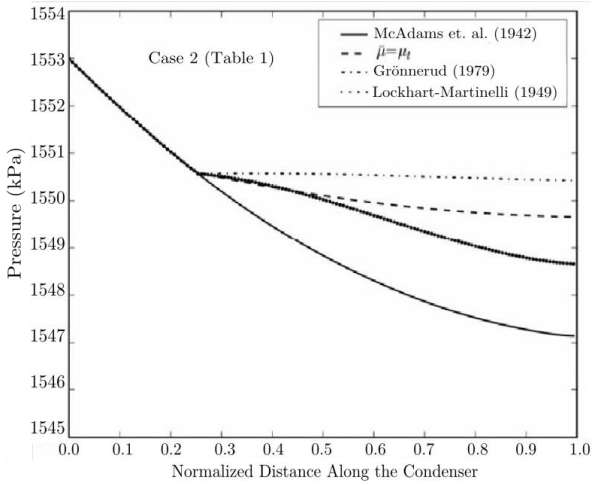

Figure 4 – Influence of F_z model on the refrigerant pressure distribution.

As can be observed in Fig. 4, the reduction in pressure in the superheated vapor region is almost linear and all the curves except that obtained by the McAdams *et al*. (1942) correlation, have a discontinuity at the beginning of saturation. It can also be noted that the total pressure loss along the condenser is very small within the 2.5 and 6 kPa (0.025 to 0.06 bar) range, according to the correlations analyzed.

It can be ascertained from Fig. 5 that the difference between the temperature profiles is negligible. Thus, the influence of the model used to evaluate the friction between the refrigerant and the tube wall is negligible and for that reason, in the present work, the procedure assuming the mean two-phase viscosity is equal to the liquid viscosity ($\bar{\mu} = \mu_l$) was adopted to determine the friction factor *f*.

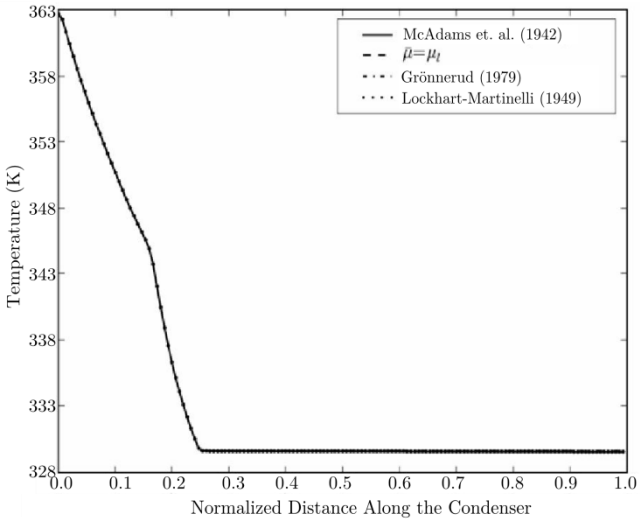

Figure 5 – Influence of F_z model on the refrigerant temperature distribution.

To evaluate the influence of the external coefficients of heat transfer by natural convection, H_e, and by radiation, H_{rad}, changes of ±20% were imposed to its initial values. Figures 6(a), 6(b) and 7 show the refrigerant temperature profiles for Case 2 (Tab. 1) when these changes are imposed to coefficients H_e, H_{rad} and (H_e + H_{rad}) respectively. It can be easily verified from Figs. 6 and 7 that the onset of condensation is delayed with the reduction of the heat transfer coefficients and advanced with the increase of these coefficients. It can also be verified that the refrigerant temperature is more sensitive to variations in H_{rad} than to variations in H_e. A -20%change in H_{rad} is found to result in a greater delay in the start of condensation than a corresponding change in H_e. Also notice the presence of subcooling liquid refrigerant around the extremities of the condenser when the values of H_e, H_{rad} and (H_e + H_{rad}) are increase by +20%.

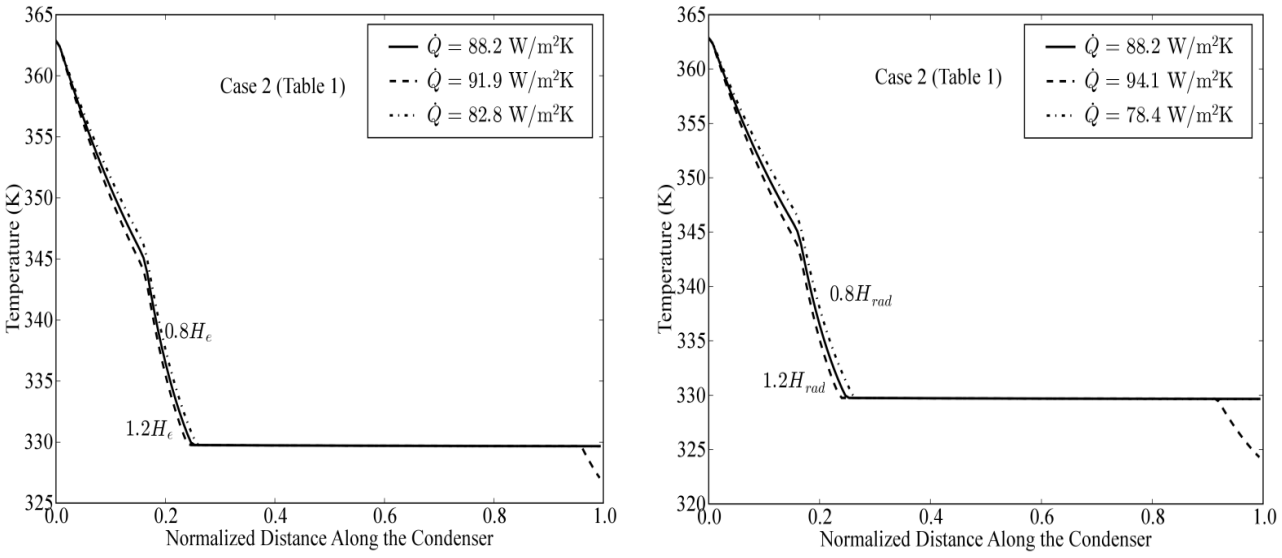

(a) (b)

Figure 6 – Refrigerant temperature profiles varying: (a) H_e in ± 20%; (b) H_{rad} in ± 20%.

Figures 6 and 7 also show the condenser capacity, $\dot{Q}$ [W]. As can be seen, when the initial values of H_{rad} and H_e are used, the condenser capacity is $\dot{Q}$ = 88.2 *W*. However, for a + 20 % and - 20% change in H_e,, the condenser capacities are found to be 91.9 *W* and 82.8 *W* respectively. Similarly, for a +20% and -20% change in H_{rad}, in, the condenser capacities are respectively 94.1 *W* and 78.4 *W*. Altering (H_e + H_{rad}) by +20% and -20% results in condenser capacities of 95.6 *W* and 72.8 *W* respectively which indicates the largest thermal resistance to radiation transfer than to natural convection heat transfer.

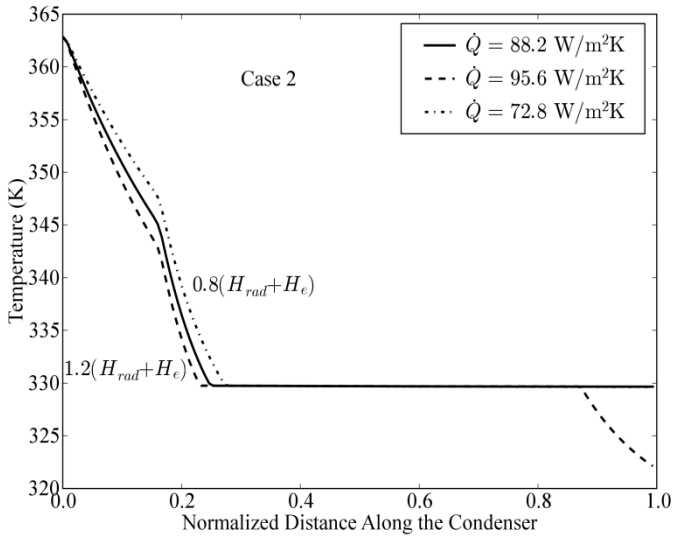

Figure 7 – Refrigerant temperature profiles varying (H_e + H_{rad}) in ± 20%.

Figure 8 shows the condensing process on a *p-h* diagram for three mass fluxes: 43.6 kg/m^{2}s, 53.4 kg/m^{2}s and 70.1 kg/m^{2}s. Notice the higher pressure drop for larger mass fluxes. However, the pressure drop does not show any significant values for all cases, reaching a maximum value of 10 kPa (0.1 bar) for a mass flux of 70.1 kg/m²s.

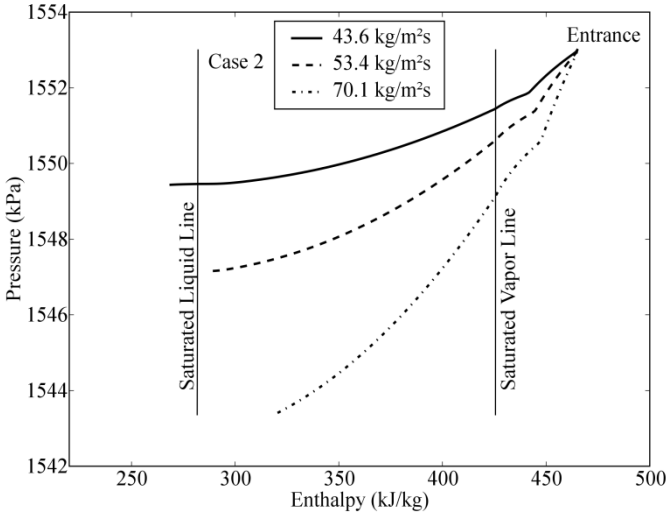

Figure 8 –*p-h* diagram for condensing process for different mass fluxes.

A reduction in the pressure drop can also be noticed in Fig. 8 toward the subcooled liquid region since its density increases as condensation of the refrigerant occurs. In the subcooled liquid region, the pressure variation is very small because the density of the liquid refrigerant is almost constant.

Table 3 shows the dimensions of two different condenser coils used in experiments conducted by Ameen *et al*. (2005). Operating conditions for the tests were: refrigerant mass flow ranging from 5x10^{-4} to 7x10^{-4} kg/s and ambient temperatures ranging from 10 to 40 ^{o}C. The refrigerant enters into the condenser in a superheated vapor state at 1.3 MPa (13 bar) and temperature of 60 ^{o}C.

Table 3 – Geometrical data of the condenser coils analyzed by Ameen *et al.* (2005).

Geometrical parameter	Condenser	
	1	2
Outer diameter (d_e) [mm]	4.9	4.9
Inner diameter(d_i) [mm]	3.28	3.28
Tube pitche (p_t) [mm]	55.4	40.9
Wire diameter (d_{wi}) [mm]	1.5	1.5
Wire pitche (p_{wi}) [mm]	6.5	7.5
Wire number	100	114
Number of coil passes	13	22
Width of the condenser (W_i) [cm]	48.7	5.31
Area of the tubes [m^2]	0.097	0.18
Area of the wires [m^2]	0.339	0.483

Figure 9 presents a comparison between results calculated using the present model and the experimental results obtained by Ameen *et al*. (2005) for the initial phase change point (IPCP). As can be observed from Fig. 9, the IPCP calculated using the present methodology is within ±20 % of the experimental values with the largest deviations concentrated in the range of 0 – 20 %.

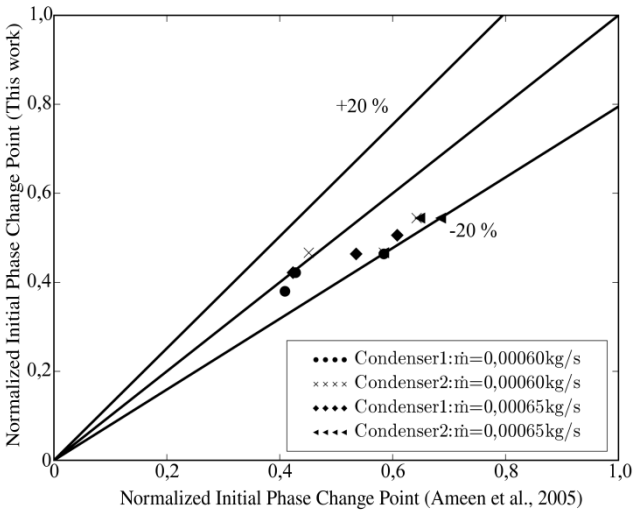

Figure 9 – Comparison between measured (Ameen *et al*. 2005) and predicted IPCP.

Comparisons between IPCP and the final phase change point (FPCP) values obtained from the present study and those measured by Ameen *et al*. (2005) are presented in Tab. 4. In the table, NSC stands for "not subcooled" flow occurrence. Notice in Tab. 4 that the greatest difference between the numerical and experimental IPCP values is 20.5% for coil 2, mass flow rate of 0.0006 kg/s and ambient temperature of 302 K while the deviations between the numerical and experimental FPCP values were even greater, attaining values above 35%.

4. TRANSIENT RESULTS

In order to analyze the transient behavior of the condenser, we consider the particular case in which, starting from the steady–state solution for a specific operating condition, the time dependent boundary conditions are imposed in accordance to (Hermes and Melo, 2008): $T_r(t) = 89{,}7 + (T_a - 89{,}7)e^{-t/10}$; $\dot{m}(t) = 1{,}78 + (9 - 1{,}78)e^{-t/5}$ and $\dot{m}(t) = 1{,}78.(1 - e^{-t/2})$, where $\dot{m}$ is the refrigerant mass flow rate and the subscripts 1 and 4 indicate the condenser inlet and outlet respectively (see Fig. 2). The geometrical parameters of the condenser used in this analysis were the same used to obtain the results presented in Tab. 2.

The temperature distributions of the refrigerant at certain instants are shown in Fig. 10. Notice that the onset of condensation moves toward the condenser outlet as the time increases. This is a result of the admission of vapor at the condenser inlet at higher temperatures as a function of time. Thus, with time, the refrigerant temperature approaches the external temperature which is assumed constant, and as a result, heat transfer diminishes, displaying the IPCP downstream. It is also observed that the temperature profiles related to instants 5 min and 15 min almost coincide.

Table 4 - Comparison between the experimental data (6) and the present numerical analysis for the phase change locations.

$\dot{m}$ [kg/s]	Coil. nº.	T_a [K]	IPCP (m)			FPCP (m)		
			Simul.	Exp.	Error (%)	Simul.	Exp.	Error (%)
0.0006	1	297	0.380	0.409	7.1	4.0	5.84	31.5
		300	0.422	0.428	1.4	4.7	6.18	23.9
		302	0.464	0.584	20.5	5.2	NSC	
	2	297	0.467	0.451	3.5	4,.9	7.06	34.9
		300	0.467	0.584	20	5.21	8.12	35.8
		302	0.545	0.642	15.1	5.84	8.63	32.3
0.00065	1	297	0.422	0.423	0.23	4.39	5.94	26.1
		300	0.464	0.535	13.3	5.06	6.22	18.6
		302	0.506	0.608	16.8	5.65	NSC	
	2	297	0.467	0.584	20	4.82	7.54	36.1
		300	0.545	0.648	15.9	5.68	8.76	35.2

Figure 11 shows the temperature distributions in transient regime at four locations along the condenser: in the condenser inlet (T1), in the wired region inlet (T2), at the center of the condenser (center of the eighth pass of the coil) (T3) and at the condenser outlet (T4). These results are found to be qualitatively similar to the experimental results of pull down testes performed by Hermes and Melo (2008) at ambient temperature of 43 ^{o}C. However, a direct comparison with the test results obtained by the aforementioned researchers was not possible because of the lack of complete information on the operating conditions employed by them.

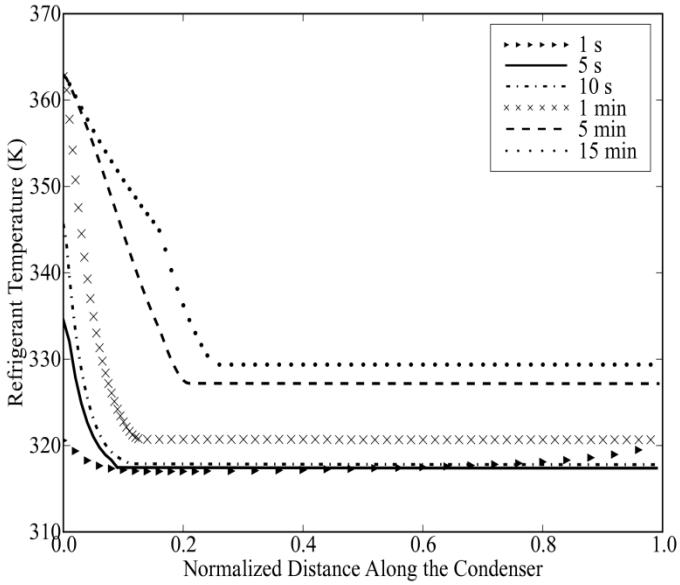

Figure 10 – Refrigerant temperature distributions at some instants in time.

As can be observed in Fig. 11, the temperature at the condenser inlet rapidly attains its steady state value, which is 362.9 K (89.7 ^{o}C). The temperature distribution in the wired inlet region (T2) is quite different from that at the condenser inlet (T1), reaching a steady state condition in about 15 min after compressor start-up (see Fig. 10). The temperature distributions at the center and at the outlet of the condenser (T3 and T4) are identical since there was no complete condensation of the refrigerant for this operating condition, as can be perceived from Fig. 10.

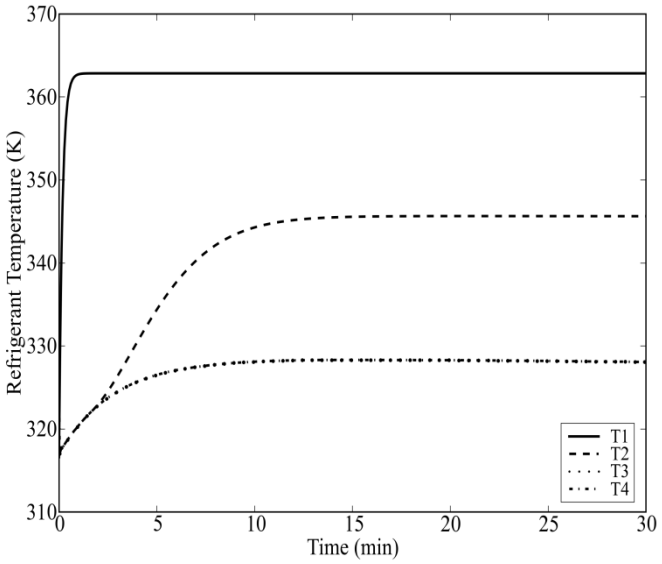

Figure 11 – Temperature distributions with time at four locations along the condenser.

5. CONCLUSIONS

This paper presents a numerical model for the simulation of one-dimensional unsteady state flows in wire-and-tube condenser commonly used in household refrigerators. The model allows prediction, in steady and unsteady states, of the refrigerant mass flow rate, pressure, quality, refrigerant and wall temperatures distributions along the tube, as a function of the heat exchanger geometry and operating conditions.

Comparisons between the results obtained by Hermes and Melo (2008) and those obtained in this work show good agreement with respect to condenser capacity, outlet temperature and outlet quality. Comparisons between the results obtained with the model and the experimental results of Ameen *et al.* (2005) demonstrated that the model underestimates the initial and final phase change points along the condenser.

As conclusion, the numerical study and the results obtained indicate the need for an improved model of the flow of air side, considering, for example, the implementation of a distributed model for the analysis of the flow and heat transfer between the tube/wires and the ambient air.

6. ACKNOWLEDGMENTS

The authors would like to acknowledge the financial support from CAPES – Coordenação de Aperfeiçoamento de Pessoal de Nível Superior which permitted the the development of this project.

7. REFERENCES

Ameen, A.; Mollik, S.A.; Mahmud, K.; Quadir, G.A.; Seetharamu, K.N., 2005, "Numerical analysis and experimental investigation into the performance of a wire-on-tube condenser of a retrofitted refrigerator", International Journal of Refrigeration, n. 26, pp. 495 – 504.

Bansal, P.K.; Chin, T.C, 2003, "Modelling and optimization of wire-and-tube condenser", International Journal of Refrigeration**,** v. 26, pp. 601-13.

Churchill, S.W., 1977, "Friction-factor equation spans all fluid-flow regimes", Chemical Engineering, v. 84, pp. 91-92.

Escanes, F.; Pérez-Segarra, C.D.; Oliva, A., 1995, "Numerical simulation of capillary-tube expansion devices, International Journal of Refrigeration", v. 18 (2), pp. 113-122.

Gnielinski, V., 1976, "New equations for heat and mass transfer in turbulent pipe and channel flow", International Chemical Engineering, v. 16, pp. 359-368.

Hermes C.J.L., Melo, C., 2008, "A first-principles simulation model for the start-up and cycling transients of household refrigerators", International Journal of Refrigeration, v. 3, pp. 1341-1357.

Klein, F.H., 1998, "Development of a Computational Code to Analyze the Performance of Household Refrigerators", MSc. thesis, Department of Mechanical Engineering, Federal University of Santa Catarina, Florianópolis-SC, Brazil, 155p. (in Portuguese).

LeFevre, E.J.; Ede, A.J., 1956, "Laminar free convection from the outer surface of a circular cylinder", Proceedings of the 9th International Congress of Applied Mechanics, Brussels, Belgium, v. 4, pp. 175-183.

Lockhart, R.W.; Martinelli, R.C., 1949, "Proposed correlation of data for isothermal two-phase two-component flow in pipes", Chemical Engineering Progress, New York, v. 45, n. 1, pp.39–48.

McAdams, W.; Woods, W,; Heroman, L., 1942, "Vaporization inside horizontal tubes", ASME Transactions, v. 64, n. 163, pp. 193-200.

McLinden, M.O.; Klein, S.A.; Lemmon, E.W.; Peskin, A.P., 1998, "Thermodynamic and Transport Properties of Refrigerants and Refrigerant Mixtures – REFPROP", National Institute of Standards and Technology – NIST, Standard Reference Database 23, Version 6.01, Gaithersburg, Maryland, USA.

Melo, C.; Arsego, C.; Maykot, R., 2004. "Experimental evaluation of wire-and-tube condensers: confining walls effect", In: 10th International Refrigeration and Air Conditioning Conference at Purdue. West Lafeyette, IN, USA.

Ould Didi, M.B.; Kattan, N.; Thome, J.R., 2002, "Prediction of two-phase pressure gradients of refrigerants in horizontal tubes", International Journal of Refrigeration, Switzerland, v. 25, n. 7, pp. 935–947.

Quadir, G.A.; Krishnan, G.M.; Seetharamu, K.N., 2002, "Modeling of wire-on-tube heat exchangers using finite element method", School of Mechanical Engineering, Malaysia, v. 38, n. 5, pp. 417-434.

Shao, D.W.; Granryd, E., 1995, "Heat transfer and pressure drop of HFC-134a – oil mixtures in a horizontal condensing tube", International Journal of Refrigeration, v. 18, n. 8, pp. 524-533.

Tagliafico, L.; Tanda, G., 1997, "Radiation and natural convection heat transfer from wire-and-tube heat exchangers in refrigeration appliances", International Journal of Refrigeration, v. 20, n. 7, pp. 461-469.

8. RESPONSIBILITY NOTICE

The authors are the only responsible for the printed material included in this paper.